Recommendation for initial stage of EISCAT_3D common programmes and their future directions

prepared by the EISCAT_3D Common Programme working group

(Version 2023-05-22)

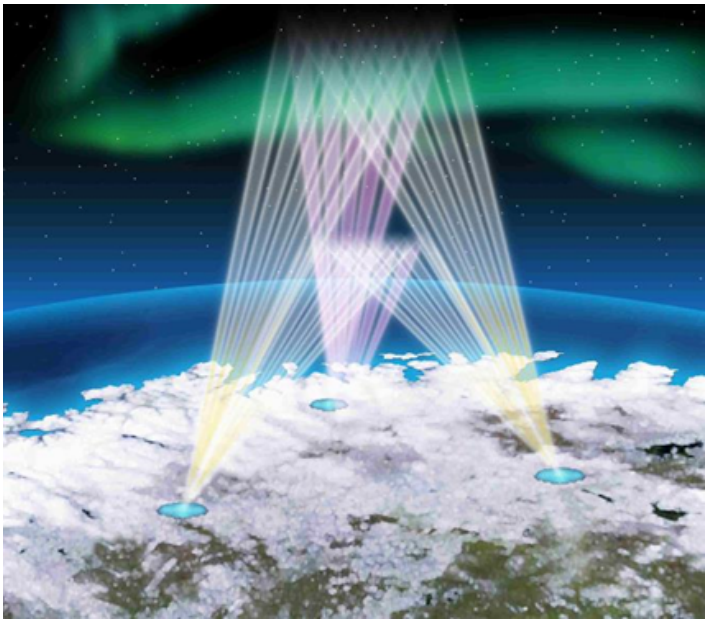

Outline

Cover art: Illustration of the EISCAT_3D multi-static observation at the 1st stage (made by NIPR).

1. Aims of this document: Yasunobu Ogawa and Andrew Kavanagh

Construction of the first stage EISCAT_3D (three sites, maximum 5 MW Tx power) has been approved by the EISCAT Council and started in September 2017. As of today, it is planned to have the system in a state for monostatic operations in late 2023, and tri-static operations will follow after developing the legal status of the EISCAT organisation. About 3.4 MW Tx power (~6700 SSPA) will be deployed in 2024. In parallel with its phased system development, test runs and initial Common Programme (CP) observations using EISCAT_3D will be started after the first light scheduled in late 2023, and the initial data will be validated. Subsequently, Special Programme (SP) observations will be conducted by researchers in the EISCAT Associates and Affiliates.

This document is intended to propose EISCAT_3D CP observations in the initial stage (2023~2025). It consists of realistic observation recommendations for the initial stage based on the experience of the EISCAT CP to date, and developmental proposals based on the high performance of the EISCAT_3D radar system. The draft recommendations will be discussed and modified in various committees and also by the EISCAT_3D user community. The recommendations will then be materialized by the EISCAT_3D software working group (SWG) and operation teams, and will be used as the initial and basic observations of the EISCAT_3D radar system.

The EISCAT Science Advisory Committee (SAC) has recommended that the EISCAT_3D SWG devotes time to ensuring that a simple analysis is available for early data from EISCAT_3D to provide standard plasma parameters (i.e. electron density, electron and ion temperature and ion velocity). The EISCAT_3D user community needs to understand that limited commissioning times mean a delay in the provision of all expected advances and data products, although EISCAT_3D will provide a number of new benefits and products as outlined in the Science Case. The SAC will provide feedback to the EISCAT_3D SWG on how the SAC and the user community can support the SWG's efforts. In this document, the draft content that the EISCAT_3D SWG intends to produce as a high priority is described in red. On the other hand, the draft content that would be better if the SAC and the user community proceed on their own initiative with the support of the SWGs is described in blue.

As described in the EISCAT Bluebook, CPs are conducted for the benefit of the entire user community, and the resulting data products are immediately available to all scientists in the countries or institutions of the EISCAT Associates and Affiliates. The current EISCAT CPs are shown in Figure 1-1, and their historical background is summarized in Wannberg (2022). CPs are often done simultaneously with other radars around the world. Such operations are scheduled through the URSI Incoherent Scatter World Days working group. The EISCAT_3D CPs will address research topics of interest to the broad EISCAT community as summarized in the EISCAT_3D Science Case (McCrea et al., 2015). In particular, continuation from the current EISCAT CP observations is important for statistical investigations including long-term EISCAT data analysis since 1981 (e.g., Ogawa et al., 2014; Bjoland et al., 2017) and comparison studies with previous interesting events (geomagnetic storms, stratospheric sudden warming events, etc.).

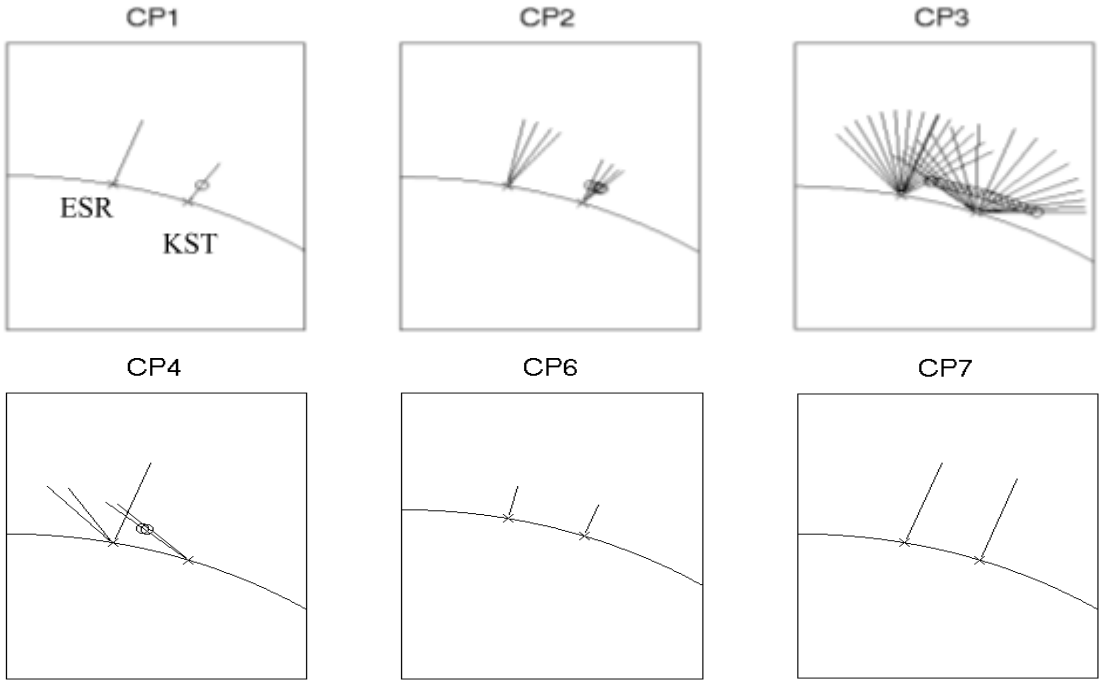

Figure 1-1: Configuration of the current EISCAT CP modes from CP-1 to CP-7. The figure is taken from the following EISCAT webpage:
https://eiscat.se/scientist/user-documentation/radar-scan-patterns/

2. Suggestions about single beam CP runs at the initial stage: Ingemar Häggström, Devin Huyghebaert and Ilkka Virtanen

2.1 Validation of new EISCAT_3D radar data.

GUISDAP has been updated for phased-array radars to accommodate multibeam radar modes in the monostatic case. As the actual format of EISCAT_3D data files is not yet set, there are some adjustments to do. For remote profiles there is still some work to do, but for the relatively narrow beams of EISCAT_3D the same approach as for the present system can be done to start with. Comparison with data with the current UHF/VHF radars to be conducted at the early stage, etc.

2.2 Pulse codes proposed for the initial CP runs

We assume that the EISCAT_3D system cannot run fully calibrated from the beginning, and a first CP should be based on the Alternating Codes (ACs). These codes are very robust, as the background is taken at the same time offset as the signal data, and have been proven to be very efficient at all CP modes for the present EISCAT systems.

2.3 Monostatic and Multi-static observations the initial CP runs (recommendation)

The first experiment to run is CP-1 mode. Since EISCAT_3D provides full vector velocity profiles the mode will also cover one of the present CP-2 objectives. The Tx power of EISCAT_3D is so high and we expect very high SNRs, but as the signal is noise-like one needs enough estimates. This can be achieved by spreading the signal over a relatively wide frequency band; that is going for short bit lengths in the code. This also enables high range resolutions. A bit length of about 1 usec should provide data of good quality down to < 1 second of integration and to achieve enough spectral resolution in the *E*-region the length of the pulse should be 700-1000 us. This leads to a 1024 x (0.75~1 usec) AC, but to start with we might go for 512 x (1.5~2 usec) pulses not to stress the system too much. Such long codes take a couple of seconds to complete, but with this high modulation 10~20 pulses are enough to suppress the ambiguities to enable good spectral data

With EISCAT_3D the remote sites produce the most important data as they measure the full profile without interruptions due to transmissions. At lower heights, they reach the full spectral resolution and at higher heights they can continue to produce quality data during transmission of the next pulse. For CP-1 the beams are spanning from 30 to ~80 degrees of elevation. Due to the geometry, the low elevation beams are wider than the high elevation ones. With some necessary overlap, this can be covered by ~35 narrow beams, which is possible with 5 or 7 wide beams divided into 7 or 5 narrow ones. With the strong sidelobes hierarchical beamforming produces, maybe 7 wide beams are needed.

All data should be sampled at 17 MHz BW to cover both up and down shifted plasma lines at all heights and at all directions. A description of the importance of measuring plasma lines for common programmes is provided in Section 4.7. The narrow band ion lines are filtered in software from this data. This leads to these numbers:

- Tx 512 bit AC, 2.5 usec bit, IPP 6.25 msec, 6.4 sec cycle, 21% duty cycle
- Rx 17 MHz BW at 1+35+35 beams, decimated to 1.25 MHz for ion lines.

2.4 Operation of the low duty-cycle modes (recommendation)

For most of the time the radar will be operated in a low power mode, and here is a

consideration for a low power CP-1, we can call it LP-1. The LP-1 should produce good enough data at all height regions from the troposphere up to the ionospheric topside. Low average power is most efficient with pulses of maximum peak power but at lower inter-pulse periods. To achieve the spectral range needed an aperiodic code is proposed. Aperiodic codes follow certain rulers, and the most known ones in radar are the Golomb rulers. Here we propose a shorter pulse than CP-1 to get to shorter pulse-to-pulse lag intervals increasing the spectral widths for the *D*-region and mixing a number of rulers makes a good shape of the lag distribution here. A simple search gave a sequence of 64 pulses spread over 384 IPPs which should be repeated to cover all alternating codes.

- Tx 128 bit AC, 5-usec bit, the shortest IPP 3.125 msec, 4*1.2 sec cycle, 3.4% duty cycle
- Transmissions at IPPs (repeated 4 times): 0 1 4 6 7 17 22 25 29 31 32 37 41 54 57 65 72 84 86 88 98 105 111 116 119 120 125 148 158 161 169 170 188 195 212 227 241 243 247 250 261 263 267 288 295 300 310 318 319 322 328 336 338 351 358 362 363 364 367 373 375 380 382 383
- Rx 17 MHz BW at 1+35+35 beams, decimated to 2.5 MHz for ion lines.

2.5 In-beam measurements for initial operations:

If it is estimated that the EISCAT_3D transmit power is 3.4 MW, and the diameter of the transmit antenna array is on the order of 42 m, the beamwidth will be approximately 1.6◦. With the full receiver array for the Skibotn site, the diameter of the receiver array is approximately 84 m, and the receiver beamwidth will be approximately 0.85◦. This will allow multiple receive beams to be simultaneously sampled from within the larger transmit beam due to the software defined radio (SDR) design of the EISCAT_3D system.

Multiple narrow receive beams can be synthesized within the transmit beam by multiplying the complex voltage samples from each of the EISCAT_3D panels by a linear phase offset. This is a simple implementation to take advantage of the EISCAT_3D capabilities to “steer” the receive beam using phased array techniques. This simple implementation is recommended for initial EISCAT_3D common programmes, and future imaging techniques can be implemented once the phased array techniques are operational and verified. An example of 5 monostatic receive beams being measured simultaneously from within the transmit beam is provided in Figure 2-1. While beams 2-5 in this configuration are not completely independent, it does allow some small-scale spatial details of the ionospheric medium to be measured. Beam 1 is included for a maximum SNR measurement where both the receive and transmit beams will have a coincident peak gain in their beam patterns.

This is also relevant for the multi-static sites, where phased receive beams will already be implemented to measure the full transmit beam for all altitudes. Due to the reduced remote receiver site array size, it is recommended to only have a single beam for each intersecting altitude during the initial Common Programme operations.

The in-beam analysis from the monostatic link will provide fine scale details of the auroral structures present, and will allow the processing of each of the receive beams independently with the existing GUISDAP software. It is expected that a new software package and processing pipeline will be implemented in the future for EISCAT_3D once the radar operations progress past the commissioning phase and are routine.

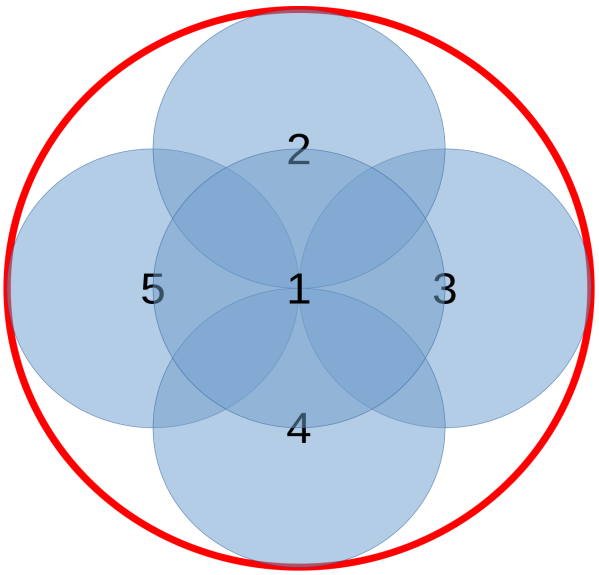

Figure 2-1: An example in-beam narrow receiver beam configuration. This assumes the receiver having half the beamwidth of the transmitter. The red circle corresponds to the transmitter beam, while the blue circles correspond to the receive beams.

3. Suggestions about multi-beam CP runs at the initial stage: Andrew Kavanagh, Yasunobu Ogawa, Dimitry Pokhotelov

3.1 Introduction

For current EISCAT observations, multi-directional observations are made by mechanically steering the antenna in elevation and azimuth. This is a relatively slow process requiring several minutes to complete a full cycle of measurements. With EISCAT_3D, data from multiple beams can be obtained simultaneously, allowing data to be analyzed at various time resolutions starting from a much lower base-line.

3.2 Suggestions for the multi-beam CP runs (recommendation)

For the initial EISCAT_3D observations, we propose to proceed with a multi-directional observation similar to the current EISCAT CP observations. The stepwise approach for the observations is shown in Table 3-1. After testing single-beam observations along the magnetic field lines or in the vertical direction, observation modes similar to the current CP-2/ip-2 and CP-3/CP-4 modes will be prepared and operated. This will allow us to determine the performance ratio with the current EISCAT VHF/UHF radars and ensure the continuity of the long-term CP data.

Based on those verifications, we will prepare an observation mode that encompasses the existing CP mode (shown as Step 4 in the Table 3-1 and Figure 3-1 (c)). In this mode, the radar beams are elliptically aligned in the north-south meridian plane, with two beams of different elevation angles in 12 azimuthal directions, allowing simultaneous observations of the *E*- and *F*-region ionosphere connected by the geomagnetic field lines (see Figure 3-2). This makes it possible to derive 3-dimensional distributions of ionospheric currents, Joule heating rates, and neutral winds at multiple points with high accuracy. Such basic parameters are highly desirable to many users working in the fields of plasma physics, aurora physics, and space weather research. For reference, the beam direction of the Step 4 is shown in Table 3-2. Note that tristatic observations would become difficult at higher latitude (> ~70 deg geographic north) because of the geometry of three site locations. Therefore, derivation of vector velocities with the monostatic method (using multi-beams) is still an essential requirement for EISCAT_3D. The beam pattern shown in the Step 4 is considered suitable for estimating the two-dimensional distribution of ion velocities in the *F*-region using Bayes' theorem based on ion velocity data at altitudes of 200-500 km [Fukizawa et al., 2024].

The Joule heating rates and, more generally, frictional heating rates, need to be measured in a wide range of altitudes across the ionospheric transition region. EISCAT measurements of the Joule heating and general frictional heating rates are essential for validating ionospheric circulation models, e.g., TIE-GCM. For studies of 3-dimensional ionospheric electrodynamics, it is essential to consider the altitude separation between Hall and Pedersen current layers. Improvements are also needed in the calculations of Pedersen and Hall conductivity values, e.g., better proxies for collision frequencies are needed.

After the establishment of the LP-1 mode described in section 2.4, multi-beam low power mode observations (e.g., the step 2 in Figure 3-1 and Table 3-1) will be prepared.

3.3 Spatial separation suitable for EISCAT_3D multi-beam CPs

Recent work by Kavanagh et al. (2022) has shown that there are differences in ion velocity derivation between single- and multi-static methods using the current EISCAT

radar, likely due to observing across different spatial and temporal scales.

These differences vary under different geomagnetic conditions and through magnetic local time and are therefore process dependent but can lead to very different estimates of energy input to the ionosphere-atmosphere system. For EISCAT_3D to play a significant role in the fundamental research that will underpin the next generation of space weather models it important to characterize the scale-based differences, that the current models may not resolve.

Given that multi-beam derivations of velocity are still desirable with EISCAT_3D, there are trade-off that must be made in terms of the angular separation and the spatial separation. The latter is important for studies of multi-scale phenomena, where a selection of spacing may be desirable, and the former is important to reduce uncertainty on horizontal measurements.

The spacing of the current CP-2 mode does quite well at achieving a balance and implementing something similar with EISCAT_3D would immediately achieve an improvement due to the simultaneous beam formation. However, ensuring that the *E*-region horizontal spacing is smaller than 100 km would be advantageous. Below 50 km it is likely that the uncertainty on the horizontal measurement increases significantly (due to high elevation angles); how much this would be remains to be seen.

With multiple beam combinations possible (as in Step 4) we can properly look at how the spatial separation really impacts the velocity derivation by selecting beams at multiple separations for intercomparison. A spread as demonstrated would be very useful in that regard. For example (depending on technical feasibility) forming multiple beams with 30 km separation in the *F* layer would allow a vector to be derived from multiple triplets of beams at 60km separation or more. This interleaving would allow the user to assess the stationarity of the local ionosphere for a given observation. For a Common Programme, such a configuration gives good coverage of the larger scale variability, which is vital. A tighter separation of beams should also be considered, which could be accomplished by nesting two modes together - something similar to case 1 but swapping with a smaller number and tighter collection of beams close to zenith to look at variability on scales of 10, 50, 100 km, 500 km (or smaller if possible).

Table 3-1: Order of preparation for Common Programme modes (recommendation)

Step	Number of beams	Equivalent to	Beam directions	Notes
1	One	CP-1	Field-aligned (FA)	AC, Monostatic first, Tristatic follows.
	One	CP-6	Vertical (VE)(Antti Kero's comment: should be Field Aligned!)	Manda pulse code (Antti Kero's comment: should be multipurpose code so that it serves wider audience)
2	Three/Five	CP-2/ip-2	see Figure 3-1 (a)	Tentative?

3	< Ten	CP-3/CP-4	see Figure 3-1 (b)	Tentative?
4	~Thirty	CP-2/-3/-4	see Figure 3-1 (c)	Different beam pattern each dump

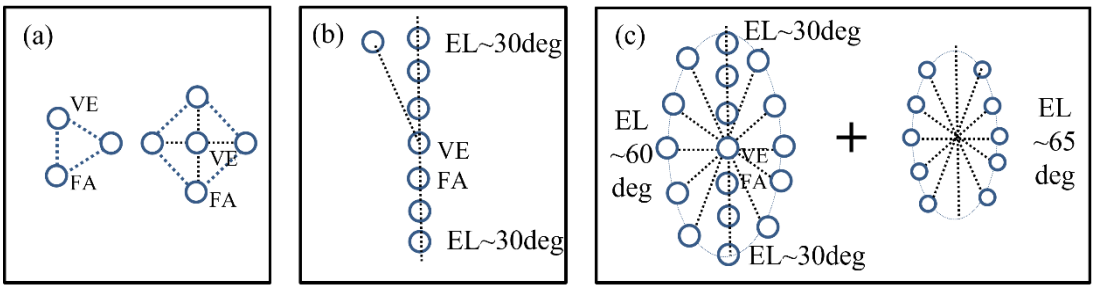

Figure 3-1: Beam patterns of the potential Common Programme modes

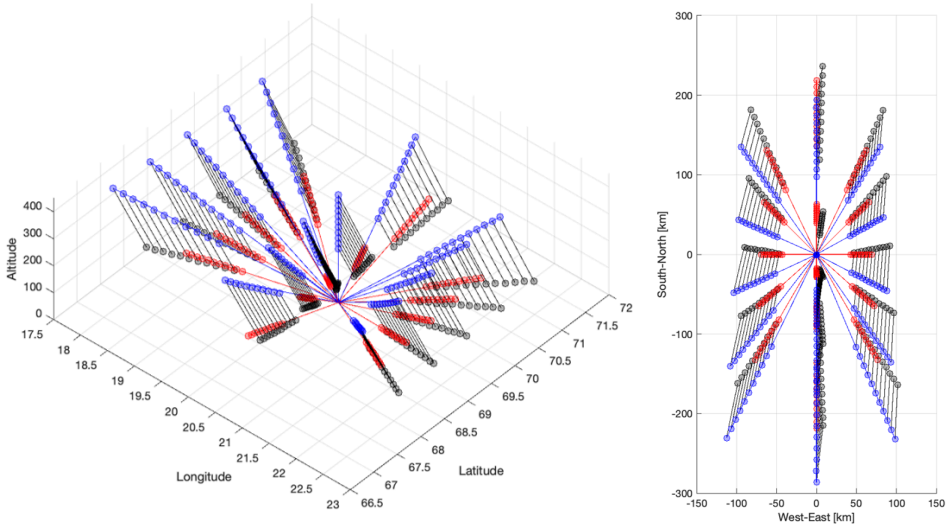

Figure 3-2: 3-dimensional configuration of the Step 4 beam pattern. Black lines indicate local magnetic field lines based on the IGRF model. The multi-beams make it possible to simultaneously observe plasma parameters in the *F*- (blue circles) and *E*- (red circles) regions on the same magnetic field lines over a wide area.

Table 3-2: Beam directions for the Step 4 every 3 cycles (every 3 dumps). We assume that the interlacing is limited up to ~10 beams (/channels).

	Ch1	Ch2	Ch3	Ch4	Ch5	Ch6	Ch7	Ch8	Ch9
AZ1 (deg)	0.0	142.5	180.0	224	0.0	116.6	180.0	243.4	189.8
EL1 (deg)	64.0	75.0	54.0	74.0	30.0	65.9.0	30.0	65.9	78.2
AZ2 (deg)	56.5	153.0	201.0	243.5	39.1	137.1	204.1	274.4	180.0
EL2 (deg)	79.0	70.5	61.0	77.5	57.6	59.5	45.6	68.1	89.9

AZ3 (deg)	123.5	163.0	212.5	297	85.6	155.9	222.9	320.9	180.0
EL3 (deg)	79.0	61.0	69.5	77.5	68.1	45.6	59.5	57.6	66.0

4. Potential usage of the initial CP data for a wide range of research subjects

Introduction

The EISCAT_3D software working group (SWG) will provide an analysis package to provide standard plasma parameters (i.e., electron density, electron/ion temperature, and ion velocity) for the initial CP data from the EISCAT_3D radar system. Ideally, it will be built on the existing GUISDAP package. Using the provided plasma parameters, various studies will be performed by numerous users. Furthermore, several researches using the initial CP data (including coherent echo signals, etc. as well as the plasma parameters) are expected to be carried out through the development and sharing of additional analysis tools, mainly by the user community, in cooperation with the EISCAT_3D SWG. A selection of those studies and observations is described in this chapter.

4.1 Modes for combined EISCAT_3D and optical observations: Björn Gustavsson

One point worth repeating is that for IS-radars the variance of our measurements decreases linearly with the number of pulses. This makes the selection of beam-modes for multi-beam experiments a compromise between number of beams to use and time-resolution of the observation-mode to reach a set variance (or equivalently between the number of beams used and the variance for a time-resolution required for the physics studied). Further for a fixed number of beams there is a trade-off between the volume probed over a beam-cycle and the beam-density.

Selecting a beam-mode/beam-configuration will always be a trade-off that has to be done weighing these requirements as best possible. For combined IS-radar and optical observations of aurora one starting-point might be to decide based on time-resolution first then number of beams and volume probed.

For the fastest intensity-variations of the aurora (for example flickering aurora with typical frequencies of up to 15 Hz) ISR observations with integration in contiguous time will be problematic even with EISCAT_3D, conditional integration (or "superimposed epoch") with synchronisation from optical intensity (See Grydeland et al. (2008)) should be possible with EISCAT_3D. For this single-beam observations in magnetic zenith are the preferred choice. This conditional integration technique works under the condition that the electron-precipitation and the ionospheric response have a modulation correlated with the flickering-intensity but are otherwise stable over time.

For combined ISR and optical studies of the fine-scale dynamics of auroral arcs where time-resolution of “one or a few tenths of a second” are acceptable it should be possible to use a couple of beams with EISCAT_3D. Since these observations typically are made in some small regions near magnetic zenith a close-packed hexagonal bundle of 7 beams could be used. For EISCAT_3D this would cover a region with a diameter of some 10 km at 100 km of altitude. This would allow rapid observations of electron-density variations and plasma-convection.

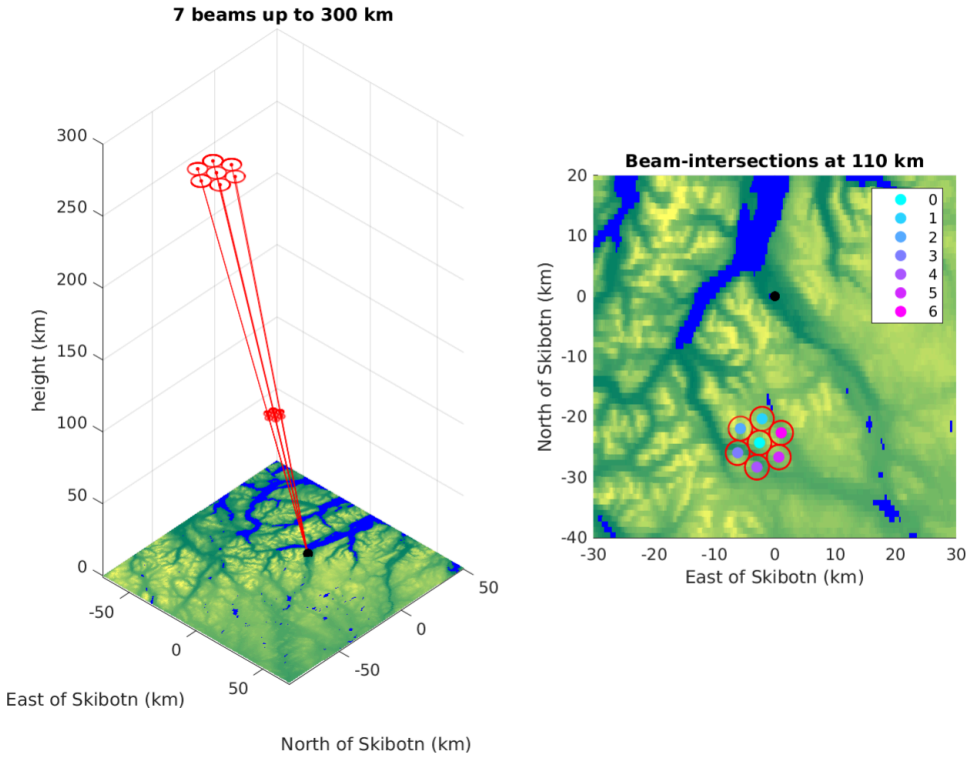

Figure 4-1: Illustration of the beams-extent for a mode with 7 beams in a close-packed hexagonal configuration around magnetic zenith with the row-orientation of the hexagon aligned with the meridian plane.

A significant consideration has to be made for the beam-scanning order. In the 7-beam configuration suggested one scan-pattern would be to transmit in the beams in a cycle 0 → 1 → 2 → 5 → 6 → 3 → 4, with the beams numbered as in Figure 4-1. This would give an equal number of pulses transmitted in the 7 pointing-directions per full cycle. However, it is possible to have use-cases where there is some level of larger interest of the observations in the field-aligned direction. This might make scan-cycles with larger numbers of pulses transmitted in beam 0 preferable. For example one could consider cycles such as: 0 → 1 → 2 → 5 → 6 → 0 → 3 → 4 → 1 → 2 → 0 → 5 → 6 → 3 → 4, which would have every 5th pulse in magnetic zenith, or 0 → 1 → 2 → 0 → 5 → 6 → 0 → 3 → 4 which would have every 3rd pulse parallel to B, or even 0 → 1 → 0 → 2 → 0→ 5 → 0 → 6 → 0 → 3 → 0 → 4. In order to fully utilise the flexibility of EISCAT_3D the possibility to choose between scan-patterns with these different preference-weightings has to be provided to the users. This type of interest-based weighting considerations should also apply for all other scan-patterns. Even for the cleanest meridian single-fan scan one researcher might require equal time-resolution/variance in all pointing-directions while another might be far more interested in, for example, the region around magnetic zenith. Finally on this side-note it is worth pointing out that we also have to figure out good scan-cycles, and as of now it is not obvious how to do this or what a good scan-cycle is.

For studies requiring observations over a larger area the observers should have the option of selecting a beam-mode that best fits their objective when it comes to the balance between time-resolution, spatial coverage and beam-density, a couple of example configurations are shown in Figures 4-2 and 4-3. For this it should be possible to offer a

number of hexagonal patterns with anywhere from 7 up to approximately 100 beams with varying spatial extent. Beams on a square grid can also be used, and should be offered to the users. For the sake of brevity only beam-modes centred around magnetic zenith are shown here, but obviously beam-modes with other geographic centres should be available.

When it comes to generating these beam-modes it is possible to generate a set of points on a hexagonal (or rectangular) grid at an altitude of choice and then calculate the corresponding pointing-directions for the beams. This would give the geometrically and geographically cleanest sampling. However, it might be preferred to generate these patterns such that "beam-fans" are aligned to be tangential to the magnetic field. This can be achieved by calculating the pointing-directions by rotating the unit-vector of the magnetic field around axes perpendicular to B - since this guarantees that we get fans of beams that lie in planes that are tangential to B. To have multiple beams in the same plane (with the magnetic field tangential to the plane) is to my understanding very beneficial for using generalized auroral tomography (e.g., Tanaka et al. (2011)) and should therefore be encouraged. Such beam-modes can either be made up of only fans of beams in some number of planes or filled in hexagonal-like patterns.

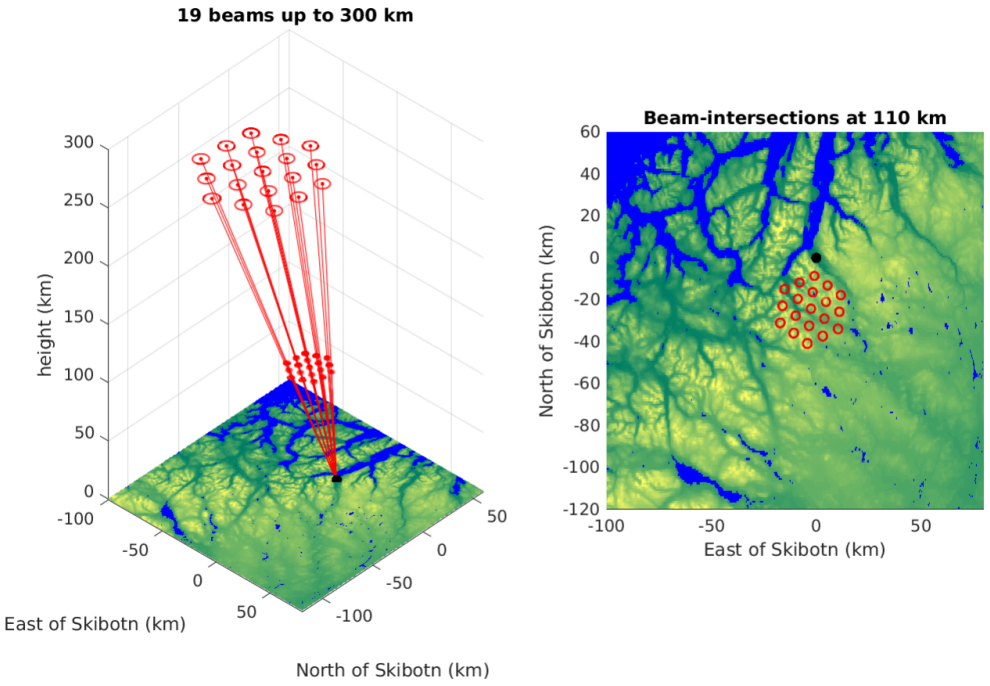

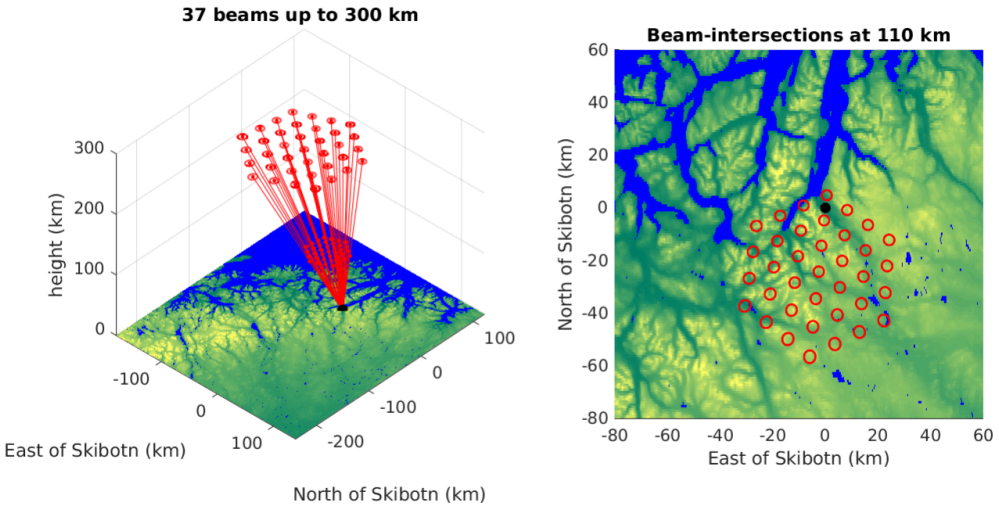

Figure 4-2: Hexagonal beam-modes with increasing number of beams, 19, 37, 61, 91 and 101, with varying spatial coverage. All configurations have one centre-row aligned with the magnetic meridian and the other 2 should be in planes nearly tangential with B.

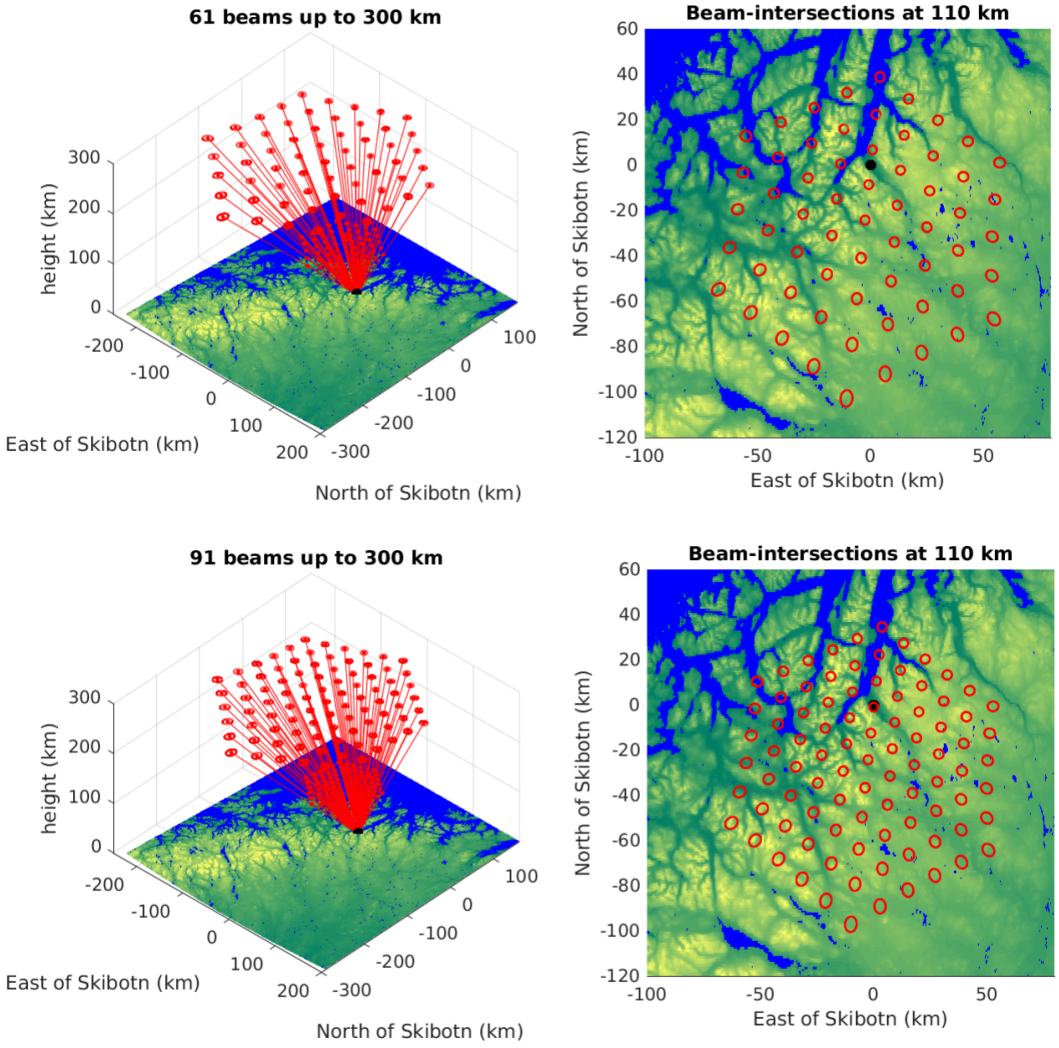

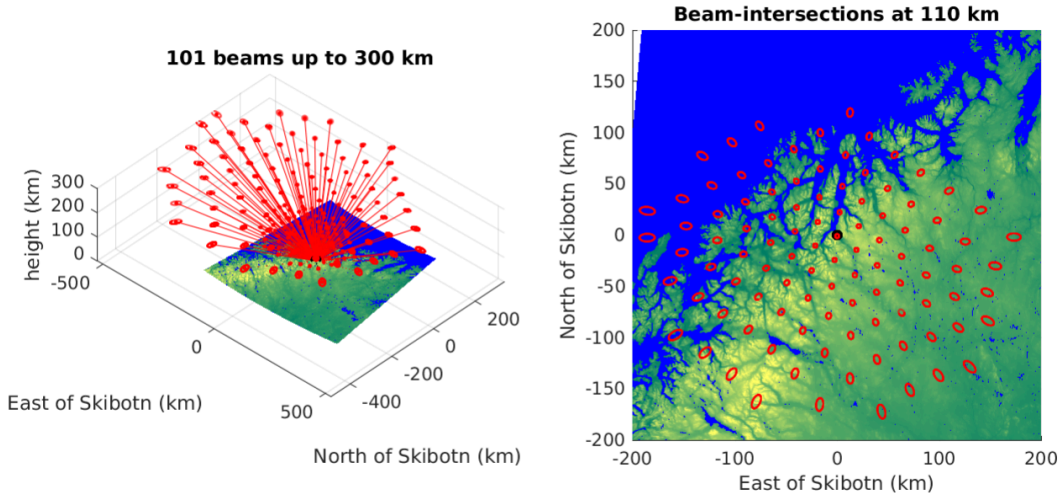

Figure 4-3: Continuation of the hexagonal beam-modes, note that the area covered with the 61 and 91 beams configurations are roughly the same with the correspondingly different beam-density and beam-cycle-time.

4.2 Coordination with satellites: Yasunobu Ogawa and Andrew Kavanagh

Coordination with scientific satellites is expected to become more active with the realization of the EISCAT_3D radar system. In the past, joint observations between the Cluster II satellites and the EISCAT radar were conducted using various Common Programme modes. Currently, coordinated observations with Swarm and ERG satellites are conducted as Special Programmes of All Associations (AA). For example, coordination with the SMILE satellite and various nano/micro-satellites is expected in the near future, and it will be necessary to regularly acquire EISCAT_3D data in the most appropriate observational modes.

For example, special mode observations such as scientific satellite/sounding rocket tracking modes with higher temporal and spatial resolution can be conducted, in parallel with CP observations of the meso-scale ionosphere over a wider area than that of current EISCAT. This would allow direct comparison of high-resolution measurements by both EISCAT_3D and satellites, and could also contribute to the calibration of satellite data.

4.3 Naturally Enhanced Ion Acoustic Lines (NEIALs): Devin Huyghebaert and Juha Vierinen

With the averaged lag-profiles provided as an output of the Common Programmes, it will be possible to further investigate naturally enhanced ion acoustic lines in the incoherent scatter measurements. These measurements fall within the ion line spectra bandwidth, and are expected to be recorded. The differences in the spectra over relatively fine spatial resolution using multiple receive beams within the larger transmit beam can be investigated.

The capability of EISCAT_3D to simultaneously measure multiple directions along the full transmit beam allows the aspect sensitivity of naturally enhanced ion acoustic lines to be investigated. The aspect sensitivity of these measurements has been performed previously with the Poker Flat Incoherent Scatter Radar (PFISR) (e.g., Akbari and Semeter, (2014)), though this was done with beam switching and some slight time offset. This can be expanded upon with EISCAT_3D, where multiple altitudes can be investigated

simultaneously from multiple directions.

4.4 Polar Mesospheric Echoes (PME): Devin Huyghebaert and Gunter Stober and Juha Vierinen

The initial Common Programme operations for EISCAT_3D will focus on using existing radar codes to probe the lower thermosphere. For *E*-region phenomena (meteors, *D*-region spectra, polar mesospheric echoes (PME)), the Manda code will commonly be used during the initial operations. With the transmit beam being larger than the receive beam for initial operations, there will be some opportunities for fine scale measurements in a small region. Each of the synthesized receive beams in this region can be independently processed with the current GUISDAP software. This will provide details on the order of kilometers within a limited region.

Both in-pulse and inter-pulse averaged lag-profiles are expected to be available. This will allow the typical small bandwidth and fine frequency resolution analysis required for *D*-region and PME spectra analysis that is available with the Manda experiments. Unfortunately it is still unclear if the raw complex data that is available during the current EISCAT Manda experiments will also be available for EISCAT_3D Manda experiments.

There will also be tri-static measurements from the 3 receiver stations available. This will provide 3-D velocity measurements along the transmit beam. Some examples of tristatic measurements with the EISCAT VHF radar that can provide a basis for what will be commonly available during Common Programme operations for PME analysis can be found in Mann et al. (2016) and Belova et al. (2018). One of the benefits of the EISCAT_3D system will be that these tristatic measurements will be available along the whole transmit beam, and not isolated to a single altitude where the remote receive beam intersects the transmit beam. This allows an altitudinal profile of the PME to be measured from multiple directions.

(4.4.1 Mesospheric coherent Radar echoes)

EISCAT_3D will also provide benchmark observations leveraging coherent radar echoes at the mesosphere and lower thermosphere such as polar mesospheric summer echoes and polar mesospheric winter echoes. Due to the high power aperture of EISCAT_3D and the ability to perform scanning experiments, it will be possible to investigate small-scale dynamical processes within these mesospheric echoes and how the scattering strength of these coherent radar signals depends on the geomagnetic activity or the background electron density. In particular, tri-static observations are suitable to derive 3D high spatially resolved winds from such echoes.

It will be advantageous to use imaging when measuring polar mesospheric echoes to obtain better resolution of these strong echoes (Chau et.al. 2020). If technically possible, the use of MIMO could be used to increase the imaging resolution.

4.5 Monitoring of meteoroid, space debris, and asteroid: Gunter Stober and Johan Kero, Juha Vierinen

Monitoring the meteor Earth Environment is an important observational capability of EISCAT_3D. Almost all observations covering the *D*-region and *E*-region altitudes will include meteor detections and, thus, it will be beneficial to implement a separate recording pipeline to extract all meteor events from the CP-mode experiments. Similar dual use data analysis was already implemented in other active phased arrays (Schult et al., 2017). Thus,

the meteor observations could leverage the complete observation time without the need to perform further dedicated meteor experiments. This will allow collecting a gigantic meteor database over time, which includes the trajectory and velocity information using the multi-receiver system of EISCAT_3D.

The advantage of EISCAT 3D is that it can provide tri-static time of flight and doppler based trajectories, which provide unambiguous trajectories. Each experiment should have a few beams pointed into the meteor altitude range in order to ensure that tri-static trajectories are obtained.

The raw voltage of the detected meteor echoes should be retained in order to allow post-processing of detected radar echoes with higher range and Doppler resolution. This will be especially important in the case of outliers, i.e., meteors that are in interstellar orbits. If raw voltage of such echoes is not available, it will be difficult to prove that the detection is not an error in the analysis program.

The EISCAT blue book allows for observations of white listed objects. Assuming these white listed objects are small radar cross-section objects and objects found in the NORAD catalog, it would be possible to analyze each radar echo for space debris. This would provide invaluable data for estimating the amount of debris in orbit, which is primarily constrained using radar measurements. Measurements of space objects can provide important information to calibrate the system as well, as there exist radar calibration spheres with well known orbits. These can help in measuring the antenna beam pattern, and to help with calibration of interferometer.

4.6 EISCAT_3D and Nordic Meteor Radar Cluster: Gunter Stober

The mesosphere and lower thermosphere is an important atmospheric region. The high variability is driven by the dynamical forcing from below and solar effects from above. EISCAT_3D and the Nordic Meteor Radar Cluster have a large common observation volume, which is ideal to investigate both processes with high spatial and temporal resolution. The Nordic Meteor Radar Cluster provides observations of neutral winds between 70-110 km altitude leveraging a recently developed 3DVAR+DIV retrieval. Temporal resolutions of a few minutes can be achieved. EISCAT_3D is able to perform optimized scanning experiments with the Nordic Meteor Radar Cluster domain, which permits investigation of ionospheric processes and disentangling the forcing from below and from above at a worldwide unprecedented temporal and spatial resolution. Furthermore, it will be possible to perform combined retrievals leveraging the 3DVAR+DIV tomographic approach from the meteor radar systems and implementing the ionospheric physics to merge EISCAT_3D data set with the meteor radar observations at the overlapping altitudes.

4.7 Plasma Lines for Calibration of EISCAT_3D Common Programmes: Devin Huyghebaert, Theresa Rexer, Björn Gustavsson, Juha Vierinen

As the capability is available, plasma line measurements should be attempted for all EISCAT 3D common mode programmes where it is possible. This involves the complex receiver voltages at large bandwidths being recorded in RAM and being processed relatively rapidly. For plasma lines at VHF, we suggest at least a 17 MHz bandwidth, which corresponds to plasma densities of up to ~ 9×10^{11} e^- /m^3 (± 8.5 MHz). This will aid in initial operations for radar calibrations, providing the plasma density values for a given altitude to be compared with the ion-line measurements.

5. Possibilities for future development of EISCAT_3D CP observations

5.1 Observations with advanced pulse codes: Ilkka Virtanen

EISCAT_3D will have the necessary flexibility in transmission and reception to use advanced pulse coding and phase coding techniques. As some of these codes cannot be decoded by traditional decoding filters but require computationally much heavier lag profile inversion (Virtanen et al., 2008), the bottleneck in taking these techniques to routine use may be in available computing power and software.

Advanced phase coding techniques that are within reach of EISCAT_3D without lag profile inversion include amplitude modulation, polyphase codes, dual polarization codes, and combinations of these. Amplitude and/or polyphase coding can be used to improve code performance in matched filtering up to the level of perfect pulse compression without sidelobes (Lehtinen et al., 2009; Roininen et al., 2014). These codes can be used as sidelobe free alternatives to the traditional Barker codes. Polyphase alternating codes (Markkanen et al., 2008) behave exactly as the traditional binary alternating codes, but can provide some benefit because they exist also in other lengths than in powers of two. Dual polarization coding (Gustavsson & Grydeland, 2009; Grydeland & Gustavsson, 2011) can be used to improve signal statistics in high SNR conditions and to shorten the alternating code cycles. A limitation of the dual polarization codes is that the polarizations are not orthogonal at the remote sites, which might limit their use to monostatic measurements.

With lag profile inversion one can perfectly decode almost arbitrary transmission modulations. This allows the design of multipurpose modulations (Virtanen et al., 2009), which consist of phase-coded pulses transmitted with variable separation between the pulses. The pulses can be arranged so that both *D*-region pulse-to-pulse correlations and *E/F*-region "intra-pulse" correlations can be measured with the same pulses. This is particularly useful in long-term monitoring type experiments (the low duty cycle mode). Lag profile inversion allows any modulation to be decoded with time resolutions not matched to the code cycle length. This resolves time resolution limitations of long alternating codes, which will affect EISCAT_3D in normal alternating code decoding.

5.2 EISCAT_3D Imaging for Common Programmes: Devin Huyghebaert

Performing in-beam imaging of the EISCAT_3D measurements will be essential to fully take advantage of the radar capabilities. It will be possible to obtain incoherent scatter spectra on relatively fine spatial scales (~100 m). A feasibility study has already been performed and published for imaging with EISCAT_3D by Stamm et al. (2021), where the scale sizes that will be observable in the electron density were investigated.

It will be possible to expand on this imaging analysis to obtain the incoherent scatter spectra in relatively fine scale over the measurement volume. This means that it will be possible to observe fine scale temperature and ion velocity structure in the volume. There must be sufficient signal to obtain these results over a reasonable averaging period. It will also be possible in the future to include plasma line imaging of the volume.

A further possibility with EISCAT_3D is to create a wider transmit beam through

appropriate phasing of the different transmit signals at each of the panels in the transmitter array. The wider beam provides an opportunity for simultaneous measurements over a large ionospheric volume by using imaging techniques. This method of analysis will be most beneficial for targets with a large scattering cross-section and power return, such as for ionospheric regions of large ionization, meteors, and polar mesospheric echoes. In the future a wide beam imaging experiment mode can be incorporated into the common programme library.

It needs to be noted that processing the EISCAT_3D data for imaging will be computationally intensive, and may take some time before being implemented for standard operations.

5.3 CP for the troposphere, stratosphere and mesosphere (MST): Evgenia Belova, Ralph Latteck

5.3.1. Introduction

There is a need for regular/quasi-continuous measurements of wind in MST in the northern Nordic area: to study waves, tropopause folds, to contribute/validate high-top atmospheric models, to validate satellite measurements of wind in TS (e.g. the current ESA Aeolus mission and forthcoming ones), to validate products of meteor radar networks, to complement the rocket campaigns etc. This need is currently and partly fulfilled by the MAARSY and ESRAD radar observations at Andoya, Norway and Esrange, Sweden, correspondingly. EISCAT_3D will provide measurements at a different location in respect to the Scandinavian mountain ridge. Due to its large power aperture, it will have better altitude coverage than conventional wind profiler radars and thus will be able to detect atmospheric echoes from the ground through the troposphere and the (lower) stratosphere. For example, the CUSAT ST radar @ 205 MHz in Cochin, India detects echoes from altitudes up to ~20 km (Mohanakumar et al, 2017) and has lower power-aperture product than it will be for EISCAT_3D.

5.3.2. Suggestions for the CP to measure three components of neutral wind in MST.

We suggest to have a new common program to measure vertical profile of a neutral wind vector over Skibotn. The method to apply is the Doppler Beam Swinging which is conventionally used for the atmospheric radars (see e.g. Latteck et al., 2012; Stober et al., 2012 for MAARSY). Since the focus would be on getting as higher as possible in the lower atmosphere, the dedicated beams with full power in at least three directions (five would be better), are preferable instead of splitting the beam within a pulse.

For the proposed MST operation modes we propose to tilt successively a full power beam in directions from the vertical: 0°, 10° N and S, 10° E and W on a pulse-to-pulse basis. The NOAA wind profiles used to use 15 degrees. Following the experience with MAARSY, we can propose different MST modes:

- Dedicated ones, i.e., with relative short IPPs, either focused on MST (e.g., 1 ms), or ST (< 0.5 ms). These modes would be ideal if interleaved with ionospheric modes (like Manda), e.g., 2 minutes of MST, 3 minutes of ionosphere and the sequence repeats every 5 minutes.
- Combined ones focused on given sequence on the MST and lower troposphere. Here

a long coded pulse and a narrow pulse, separated by ~0.8 ms are used, with the sequence repeated every 1 ms.

- Combined with ionospheric modes, where all altitudes are measured at the same time (an aperiodic code is a possible example).

Coherent integrations should be avoided if possible or kept to a necessary minimum. We propose to realize this flexibility in software rather than hardware, i.e., to use coherent integration later in the analysis depending on the altitude of interest, and to keep the raw data flexible and as high-resolution as possible.

For the simple modes a tool for the visualisation of the vertical profiles of wind velocity in RT or near real time will be very desirable.

5.4 Modes for EISCAT_3D observations for Heating experiments: Björn Gustavsson

For EISCAT_3D observations during Heating-experiments bespoke beam-modes should also be available. For observing along the magnetic-field-line of Heating at *F*-region heights from 180 to 350 km it should be sufficient with five beams in a tight fan. For observing the entire main-lobe for experiments with Heating transmitting with array 2 at 4 MHz 37-61 beams in a hexagonal bundle should be enough to cover the -3 dB full-width. For *D*-region heating-experiments it should be enough to cover the main-lobe of Heating with 19 beams in a hexagonal pattern (see Figure 5-1). Further beam-modes should be available for Heating-experiments with transmission in at least magnetic zenith in the vertical direction. Further, since the response is strong coverage out into the first side-lobes will eventually become interesting - which obviously require larger spatial coverage.

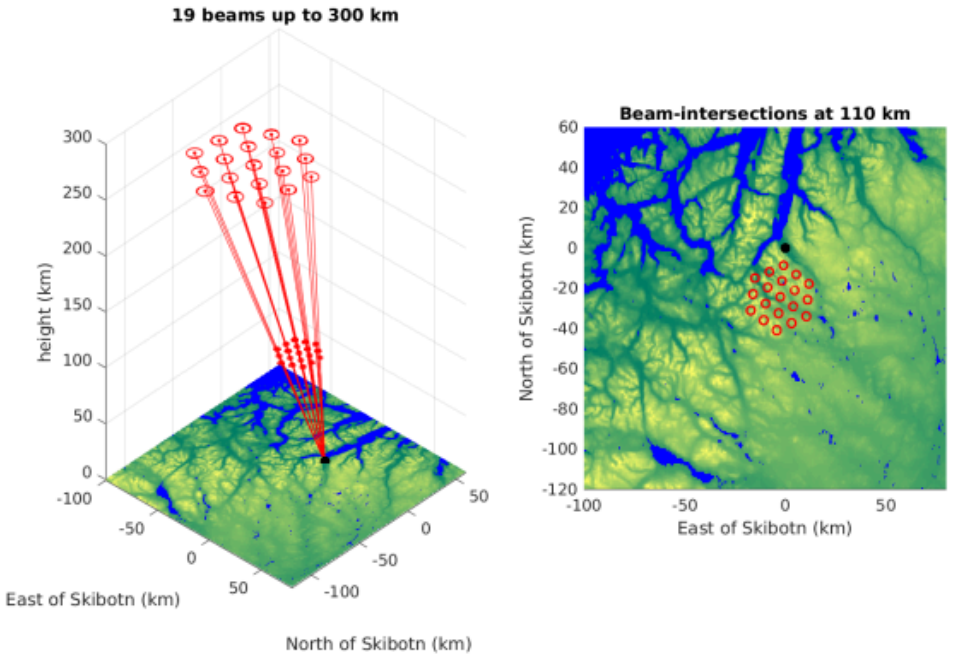

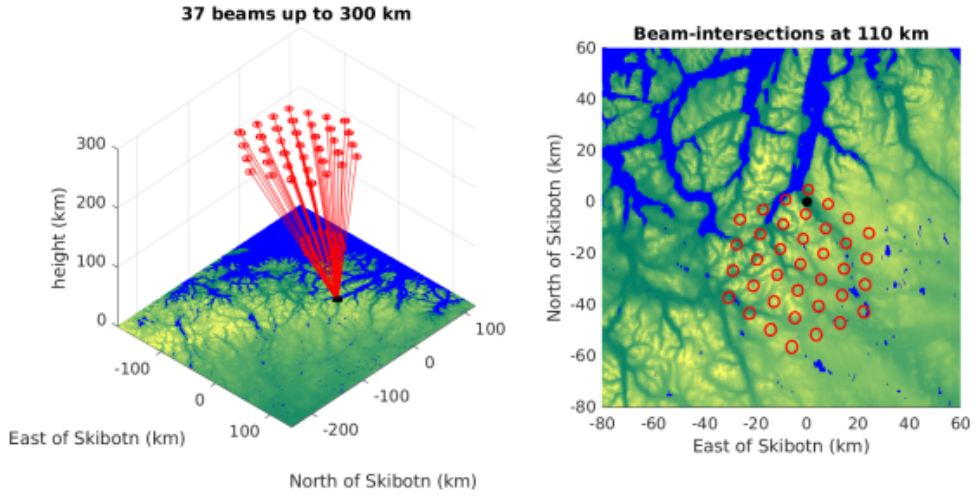

Figure 5-1: Hexagonal beam-modes with increasing number of beams, 19, 37, 61, 91 and 101, with varying spatial coverage. All configurations have one centre-row aligned with the magnetic meridian and the other 2 should be in planes nearly tangential with *B*.

5.5 Additional Beam-scan-modes: Björn Gustavsson, Andrew Kavanagh, and Yasunobu Ogawa

In order to make it feasible for the most casual of EISCAT_3D users to utilize the multiple-beams capacity the system should be set up such that the operating scientist can simply pick and choose from a graphical menu – this should be no more difficult than ordering food from a restaurant menu. With time some tools for designing beam-modes and scan-sequences should be developed, too.

In this section an outline of such a menu is presented. This is just included to illustrate how easy it should be for a user to select a suitable beam-mode to give the best observations for the observations attempted. This is also a small illustrating example – additional modes, or modifications and adaptions should be included, for example the single-fan-mode included here should be complemented with fans scanning over a wider range of zenith-angles, in both directions and further north and south respectively (see Figure 5-2, and 5-3).

In addition, the EISCAT_3D mode with multiple equally spaced beams (e.g. 5 x 5) with good time resolution would be a great improvement for atmospheric gravity wave research in terms of the possibility to measure wave structures. For example, such observations could first be performed as SPs, and after some trial and error with grid spacing, number of beams, etc., it could be incorporated into the CP and run quite frequently.

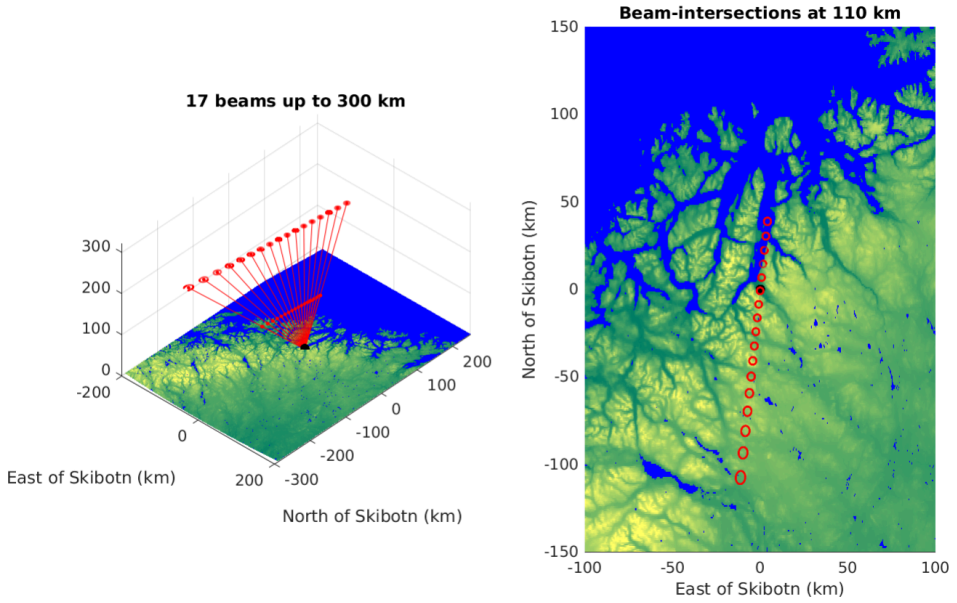

Figure 5-2: 1 fan-beam mode: fan-1-Bsym-medium

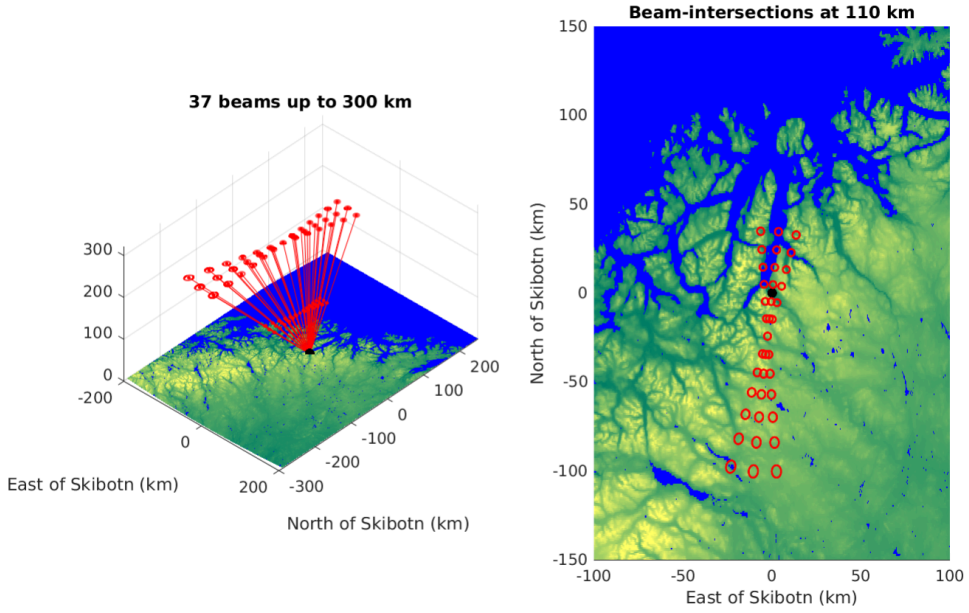

Figure 5-3: 3 fan-beam mode: fan-3-Bsym-medium

(Note: removed most of the figures at this stage.)

5.6 Advantages/disadvantages of randomly sampling beams: Gunter Stober, Dimitry Pokhotelov, Florian Guenzkofer, et al.

EISCAT_3D opens entirely new opportunities to perform scanning experiments using various scanning strategies. Similar multi-beam scans have been already implemented in other phase arrays such as MU-Radar, PFISR, or MAARSY. These scanning strategies always is a compromise between the required variance that is accepted to analyze the spectra and the temporal resolution of the process that is intended to be

investigated (Worthington, et al. 1999, Nicolls et al., 2007, Sommer et al., 2016). Random sampling is best suited for more incoherent processes that can be statistically described by white noise, whereas systematic multi-beam selections permit to use a priori knowledge about the spatial coherence to correct for temporal offsets between different scanning regions, which permits tracking coherent structures through the entire observation volume (Stober et al., 2014, 2018). In summary, the biggest advantage of random sampling is the coverage of a large observation volume with a short revisiting time between different sequential multi-beam experiments compared to a more systematic and regular scanning pattern. However, systematic and regular scans provide the benefit to remove the temporal offset between each sequential scan under the assumption of some spatial coherence within the observation volume.

Such aspects are also worth considering for all in-beam imaging techniques such as CAPON or Max-Entropy, which require multi-receiver techniques. The quality of the imaging depends on the recorded data. Typically, small sub-arrays out of the main array are correlated or recombined with phase shifts to perform post-beam steering in software on reception. However, as each of these smaller sub-arrays shows an increased variance, it might require collecting longer time series or more pulses for each beam direction, which increases the dwell time for each beam or scan sequence and, thus, the overall scanning time is increased as well. Again, there is a compromise needed between the temporal resolution that is required to study a certain process and the ability to infer small-scale spatial information. Furthermore, the total power can be corrected by the deconvolved antenna pattern from the software image compared to the standard beam forming.

5.7 Future Directions for Plasma Lines with EISCAT_3D:

Devin Huyghebaert, Theresa Rexer, Björn Gustavsson, Juha Vierinen

For large plasma densities (> 10^{12} m^{-3}), the receive bandwidth would need to be increased from the value of 17 MHz mentioned earlier or the center frequency of the receiver would have to be shifted from the transmit frequency. The shifted receiver center frequency mode could be for specialized programs more so than common programmes, and would result in only one of the plasma lines to be measured. In this case the plasmaline with the least noise should be selected.

An example of the measurement capabilities for plasma lines using large bandwidth radio receivers is provided in Figure 4-4. The data was measured during daytime conditions using the Arecibo incoherent scatter radar, providing high resolution details about the ionospheric plasma density over most of the altitudinal profile at 150 m resolution. While the sensitivity and frequency of Arecibo are more optimized for these plasma line measurements, similar signal processing efforts should be made with EISCAT 3D to obtain plasma line profiles on a regular basis.

It is expected that the raw high-bandwidth complex voltage data will not be available for users for experiments. It is therefore recommended that some pre-recorded high-bandwidth data with plasma lines are approved for the user community for plasma line tool development. This will allow users to develop plasma line processing tools that can be implemented in the signal processing chain by EISCAT for EISCAT 3D. The expectation is that the plasma line data will either be averaged auto-correlation functions with a significant number of lags, which could result in significant data

storage requirements, or the derived plasma line parameters from analysis tools developed by EISCAT and/or the community. An end goal would be the implementation of automatic plasma line detection and derivation of parameters in the data for all common programme experiments.

Figure 4-4: Example of plasma lines measured by the Arecibo incoherent scatter radar. The y-axis corresponds to the altitude, while the x-axis corresponds to the frequency of the signal. The greyscale is the signal-to-noise ratio (SNR). Contributed by Juha Vierinen.

Assuming the plasma lines can be measured, this would be great for calibration of the electron densities and temperatures measured by EISCAT 3D. The two examples of electron density calculation from plasma lines compared to ion lines, given in Figure 4-5, indicate this for E- and F-region measurements. While these measurements were made at different frequencies than EISCAT 3D will operate at, they highlight the increase in electron density measurement accuracy that is obtained through plasma line analysis. An excellent summary and review of the measurement of plasma lines with incoherent scatter radars is provided by Akbhari et al. (2017).

EISCAT 3D has the capability to make measurements of both the up- and down-shifted plasma lines with its large receiver bandwidth. There has been work done previously on using the up- and down- shifted plasma lines to obtain electron velocities independent of the ion velocities (e.g., Guio and Lilensten (1999) and Nicolls et al. (2006)). With EISCAT 3D, the velocities can be determined in 3-dimensions, providing full vectors of the ion and electron velocities and direct measurements of the ionospheric currents.

It should be noted that there may be issues with noise in the radio bands of interest, but this does not mean we should not plan to make these measurements. Even having one of either the up- or down- shifted plasma lines will significantly increase the accuracy of EISCAT 3D measurements.

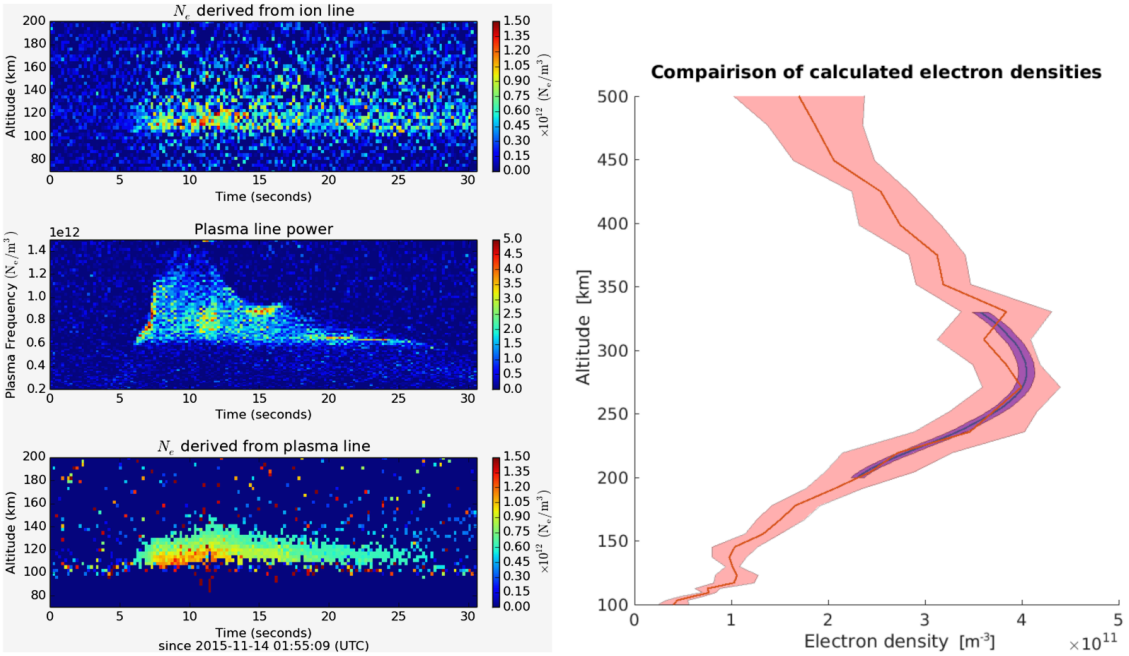

Figure 4-5: (left) (top) Electron density profile estimated from ion line power. (middle) Maximum plasma line power across all altitudes. (bottom) Electron density profile associated with auroral precipitation derived from the plasma line. Measurements were made by the Sondrestrom incoherent scatter radar. (from Vierinen et al. (2016))
(right) Altitude profile of electron density calculated from the ion line and plasma line spectra obtained from the UHF EISCAT radar. The red (ion line) and blue (plasma line) shaded areas show the uncertainty calculated for each. (from Rexer et al. (2018))

6. References

Akbari, H. and Semeter, J. L. (2014). Aspect angle dependence of naturally enhanced ion acoustic lines. Journal of Geophysical Research: Space Physics 119, 5909–5917. doi: https://doi.org/10.1002/2014JA019835

Akbari, H., Bhatt, A., La Hoz, C. et al. Incoherent Scatter Plasma Lines: Observations and Applications. Space Sci Rev 212, 249–294 (2017). https://doi.org/10.1007/s11214-017-0355-7

Belova, E., Kawnine, M., Haggstrom, I., Sergienko, T., Kirkwood, S., and Tjulin, A. (2018). Tristatic observation of polar mesosphere winter echoes with the EISCAT VHF radar on 8 January 2014: a case study. Earth, Planets and Space 70, 110. doi: https://doi.org/10.1186/s40623-018-0878-5

Bjoland, L. M., Y. Ogawa, C. Hall, M. Rietveld, U.P. Lovhaug, C. La Hoz, H. Miyaoka (2017), Long-term variations and trends in the polar E-region, Journal of Atmospheric and Solar-Terrestrial Physics, Volume 163, Pages 85-90, doi: 10.1016/j.jastp.2017.02.007.

Bluebook 2015 - EISCAT Scientific Association, https://eiscat.se/wp-content/uploads/2017/06/BlueBook_Edition2015.pdf

Chau JL, Urco JM, Avsarkisov V, Vierinen JP, Latteck R, Hall CM, Tsutsumi M. Four‐dimensional quantification of Kelvin‐Helmholtz instabilities in the polar summer mesosphere using volumetric radar imaging. Geophysical Research Letters. 2020 Jan;47(1):e2019GL086081.

Fukizawa, M., Y. Ogawa, K. Nishimura, G. Ueno, T. Nishiyama, T. Hashimoto, T. Tsuda, Feasibility study to estimate the ion velocity field in the F region from EISCAT_3D radar observations, EGU General Assembly 2024, EGU24-7480, 2024.

Grydeland, T., B. Gustavsson, L. Baddeley, J. Lunde, and E. M. Blixt (2008), Conditional integration of incoherent scattering in relation to flickering aurora. J. Geophys. Res., 113:A08305,. doi: 10.1029/2008JA013039.
URL http://www.agu.org/pubs/crossref/2008/2008JA013039.shtml.

Grydeland, T. and B. Gustavsson (2011), Orthogonal-polarization multipulse sequences, Radio Science, 46, RS1003, doi:10.1029/2010RS004425

Guio, P., Lilensten, J. Effect of suprathermal electrons on the intensity and Doppler frequency of electron plasma lines. Annales Geophysicae 17, 903–912 (1999). https://doi.org/10.1007/s00585-999-0903-x

Gustavsson, B. and T. Grydeland (2009), Orthogonal polarization alternating codes, Radio Science, 44, RS6005, doi: 10.1029/2008rs004132

Kavanagh, A., Y. Ogawa, E. E. Woodfield (2022), Two techniques for determining F-region Ion Velocities at meso-scales: differences and impacts on Joule heating, *Journal of Geophysical Research: Space Physics*, doi:10.1029/2021JA030062.

Latteck, R., Singer, W., Rapp, M., Vandepeer, B., Renkwitz, T., Zecha, M., and Stober, G. (2012), MAARSY: The new MST radar on Andøya—System description and first results, Radio Sci., 47, RS1006, doi:10.1029/2011RS004775.

Lehtinen, M., B. Damtie, P. Piiroinen, and M. Orispää (2009), Perfect and almost perfect pulse compression codes for range spread radar targets, Inverse Problems and Imaging, 3 (3), 465-486, doi:10.3934/ipi.2009.3.465

Mann, I., Haggstrom, I., Tjulin, A., Rostami, S., Anyairo, C. C., and Dalin, P.(2016). First wind shear observation in PMSE with the tristatic EISCAT VHF radar. Journal of Geophysical Research: Space Physics 121, 11,271–11,281. doi:

https://doi.org/10.1002/2016JA023080
McCrea, I. W., A. Aikio, L. Alfonsi, E. Belova, S. Buchert, M. Clilverd, N. Engler, B. Gustavsson, C. Heinselman, J. Kero, M. Kosch, H. Lamy, T. Leyser, Y. Ogawa, K. Oksavik, A. Pellinen-Wannberg, F. Pitout, M. Rapp, I. Stanislawska, J. Vierninen (2015), The science case for the EISCAT_3D radar, Progress in Earth and Planetary Science, doi:10.1186/s40645-015-0051-8.
Markkanen, M., J. Vierinen, and J. Markkanen (2008), Polyphase alternating codes, Annales Geophysicae, 26, 2237-2243, doi: 10.5194/angeo-26-2237-2008
Mohanakumar, K., Kottayil, A., Anandan, V. K., Samson, T., Thomas, L., Satheesan, K., Rebello, R., Manoj, M. G., Varadarajan, R., Santosh, K. R., Mohanan, P., & Vasudevan, K. (2017). Technical Details of a Novel Wind Profiler Radar at 205 MHz, Journal of Atmospheric and Oceanic Technology, 34(12), 2659-2671.
Nicolls, M. J., Sulzer, M. P., Aponte, N., Seal, R., Nikoukar, R., and González, S. A. (2006), High-resolution electron temperature measurements using the plasma line asymmetry, Geophys. Res. Lett., 33, L18107, doi:10.1029/2006GL027222.
Nicolls, M. J., Heinselman, C. J., Hope, E. A., Ranjan, S., Kelley, M. C., and Kelly, J. D. (2007), Imaging of Polar Mesosphere Summer Echoes with the 450 MHz Poker Flat Advanced Modular Incoherent Scatter Radar, Geophys. Res. Lett., 34, L20102, doi:10.1029/2007GL031476.
Ogawa, Y., T. Motoba, S. C. Buchert, I. Häggström, S. Nozawa (2014), Upper atmosphere cooling over the past 33 years, Geophys. Res. Lett., 41, 5629-5635, doi:10.1002/2014GL060591.
Rexer, T., Gustavsson, B., Leyser, T., Rietveld, M., Yeoman, T., & Grydeland, T. (2018). First observations of recurring HF-enhanced topside ion line spectra near the fourth gyroharmonic. Journal of Geophysical Research: Space Physics, 123, 8649–8663. https://doi.org/10.1029/2018JA025822
Roininen, L., M.S. Lehtinen, P. Piiroinen, and I.I. Virtanen (2014), Perfect radar pulse compression via unimodular Fourier multipliers, Inverse Problems and Imaging, 8 (3), 831-844, doi: 10.3934/ipi.2014.8.831
Schult, C., Gunter Stober, Diego Janches, Jorge L. Chau (2017), Results of the first continuous meteor head echo survey at polar latitudes, Icarus, Volume 297, Pages 1-13, ISSN 0019-1035, https://doi.org/10.1016/j.icarus.2017.06.019.
Sommer, S., Stober, G., and Chau, J. L. (2016), On the angular dependence and scattering model of polar mesospheric summer echoes at VHF, J. Geophys. Res. Atmos., 121, 278– 288, doi:10.1002/2015JD023518.
Stamm, J., Vierinen, J., Urco, J. M., Gustavsson, B., and Chau, J. L. (2021). Radar imaging with EISCAT 3D. Annales Geophysicae 39, 119–134. doi:10.5194/angeo-39-119-2021
Stober, G., Latteck, R., Rapp, M., Singer, W., and Zecha, M.: MAARSY – the new MST radar on Andøya: first results of spaced antenna and Doppler measurements of atmospheric winds in the troposphere and mesosphere using a partial array, Adv. Radio Sci., 10, 291–298, https://doi.org/10.5194/ars-10-291-2012, 2012.
Tanaka, Y. M., T. Aso, B. Gustavsson, K. Tanabe, Y. Ogawa, A. Kadokura, H. Miyaoka, T. Sergienko, U. Brandstrom, and I. Sandahl (2011), Feasibility study on Generalized-Aurora Computed Tomography. Annales Geophysicae, 29(3): 551–562. ISSN 0992-7689. doi:10.5194/angeo-29-551-2011.
Vierinen, J., Bhatt, A., Hirsch, M. A., Strømme, A., Semeter, J. L., Zhang, S.-R., and

Erickson, P. J. (2016), High temporal resolution observations of auroral electron density using superthermal electron enhancement of Langmuir waves, Geophys. Res. Lett., 43, 5979– 5987, doi:10.1002/2016GL069283.

Virtanen, I.I., Lehtinen, M.S., T. Nygrén, M. Orispää, and J. Vierinen (2008), Lag profile inversion method for EISCAT data analysis, Annales Geophysicae, 26, 571-581, doi: 10.5194/angeo-26-571-2008

Virtanen, I.I., J. Vierinen, and M.S. Lehtinen (2009), Phase-coded pulse aperiodic transmitter coding, Annales Geophysicae, 27, 2799-2811, doi: 10.5194/angeo-27-2799-2009

Virtanen, I. I., McKay-Bukowski, D., Vierinen, J., Aikio, A., Fallows, R., and Roininen, L. (2015), Plasma parameter estimation from multistatic, multibeam incoherent scatter data, J. Geophys. Res. Space Physics, 119, pages 10,528– 10,543. doi:10.1002/2014JA020540.

Wannberg, G. (2022), History of EISCAT – Part 5: Operation and development of the system during the first 2 decades, Hist. Geo Space. Sci., 13, 1–21. https://doi.org/10.5194/hgss-13-1-2022

Worthington, R. M., Palmer, R. D., and Fukao, S. (1999), Letter to the Editor: Complete maps of the aspect sensitivity of VHF atmospheric radar echoes, Ann. Geophys., 17, 1116–1119, https://doi.org/10.1007/s00585-999-1116-z.

7. Members of the EISCAT_3D Common Programme working group

Yasunobu Ogawa (NIPR, Japan) from the EISCAT Scientific Advisory Committee
Andrew Kavanagh (BAS, UK) from the EISCAT Scientific Advisory Committee
Ralph Latteck (IAP, Germany) from the EISCAT Scientific Advisory Committee
Ingemar Häggström (EISCAT HQ, Sweden)
Johan Kero (IRF, Sweden)
Björn Gustavsson (UiT, Norway)
Devin Huyghebaert (UiT, Norway)
Juha Vierinen (UiT, Norway)
Ilkka Virtanen (Univ. of Oulu, Finland)
Dimitry Pokhotelov (DLR, Germany)
Florian Guenzkofer (DLR, Germany)
Gunter Stober (IAP, Germany)
Mizuki Fukizawa (NIPR, Japan)